Figure S1.

A)

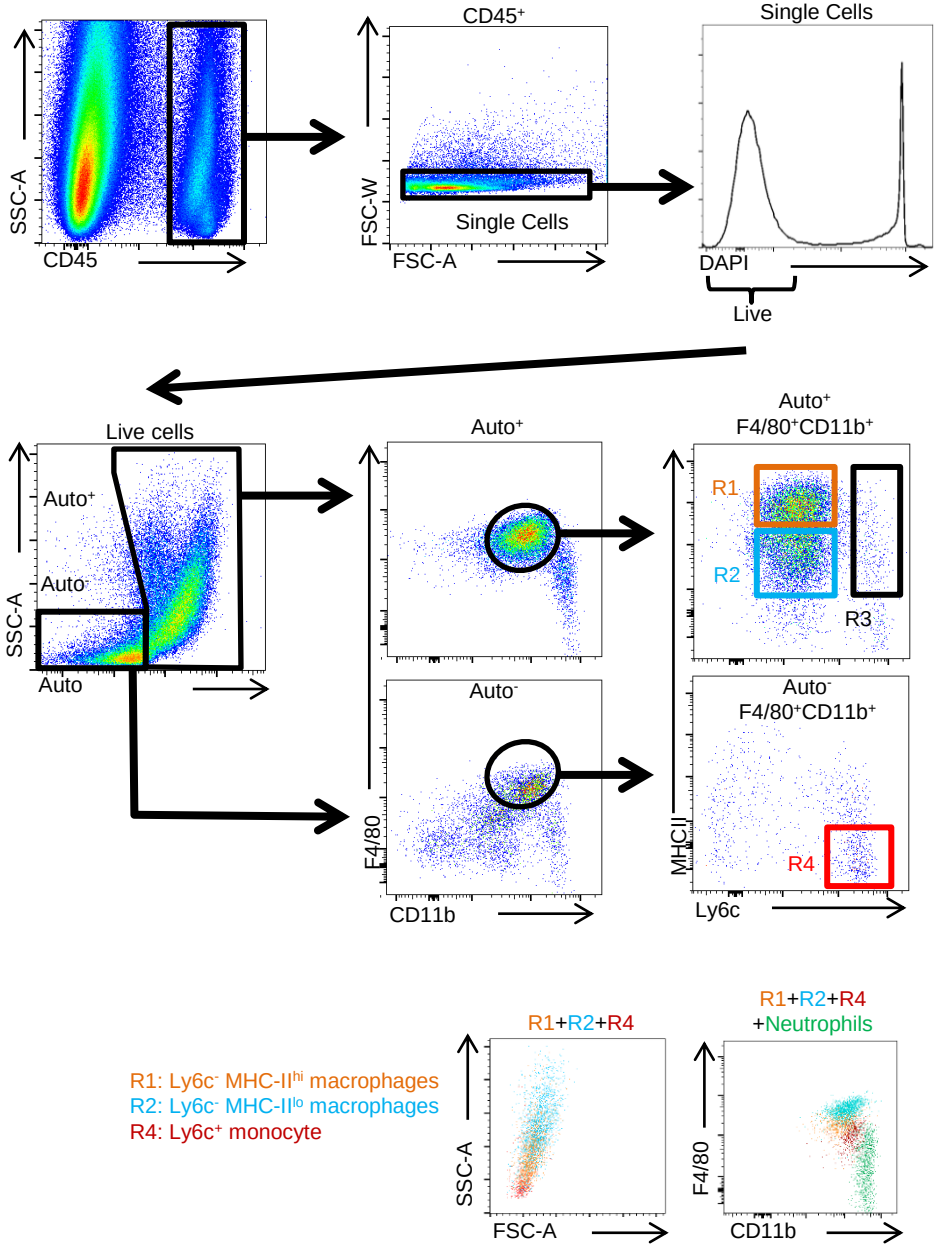
SSC-A
CD45
CD45+
FSC-W
Single Cells
FSC-A
Single Cells
DAPI
Live
Live cells
Auto+
Auto-
SSC-A
Auto
Auto+
Auto-
F4/80
CD11b
Auto+
F4/80+CD11b+
R1
R2
R3
Auto-
F4/80+CD11b+
MHCII
R4
Ly6c
R1: Ly6c- MHC-IIhi macrophages
R2: Ly6c- MHC-IIlo macrophages
R4: Ly6c+ monocyte
R1+R2+R4
SSC-A
FSC-A
R1+R2+R4
+Neutrophils
F4/80
CD11b

B)

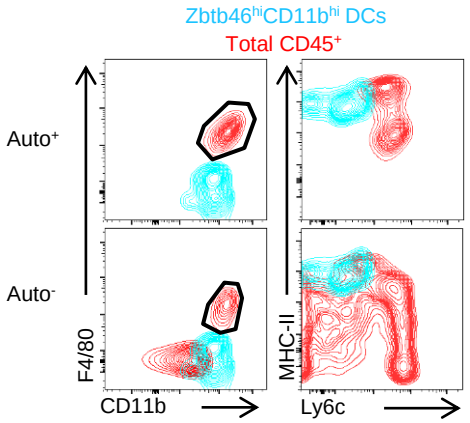
Zbtb46hiCD11bhi DCs
Total CD45+
Auto+
Auto-
F4/80
CD11b
MHC-II
Ly6c

Figure S2.

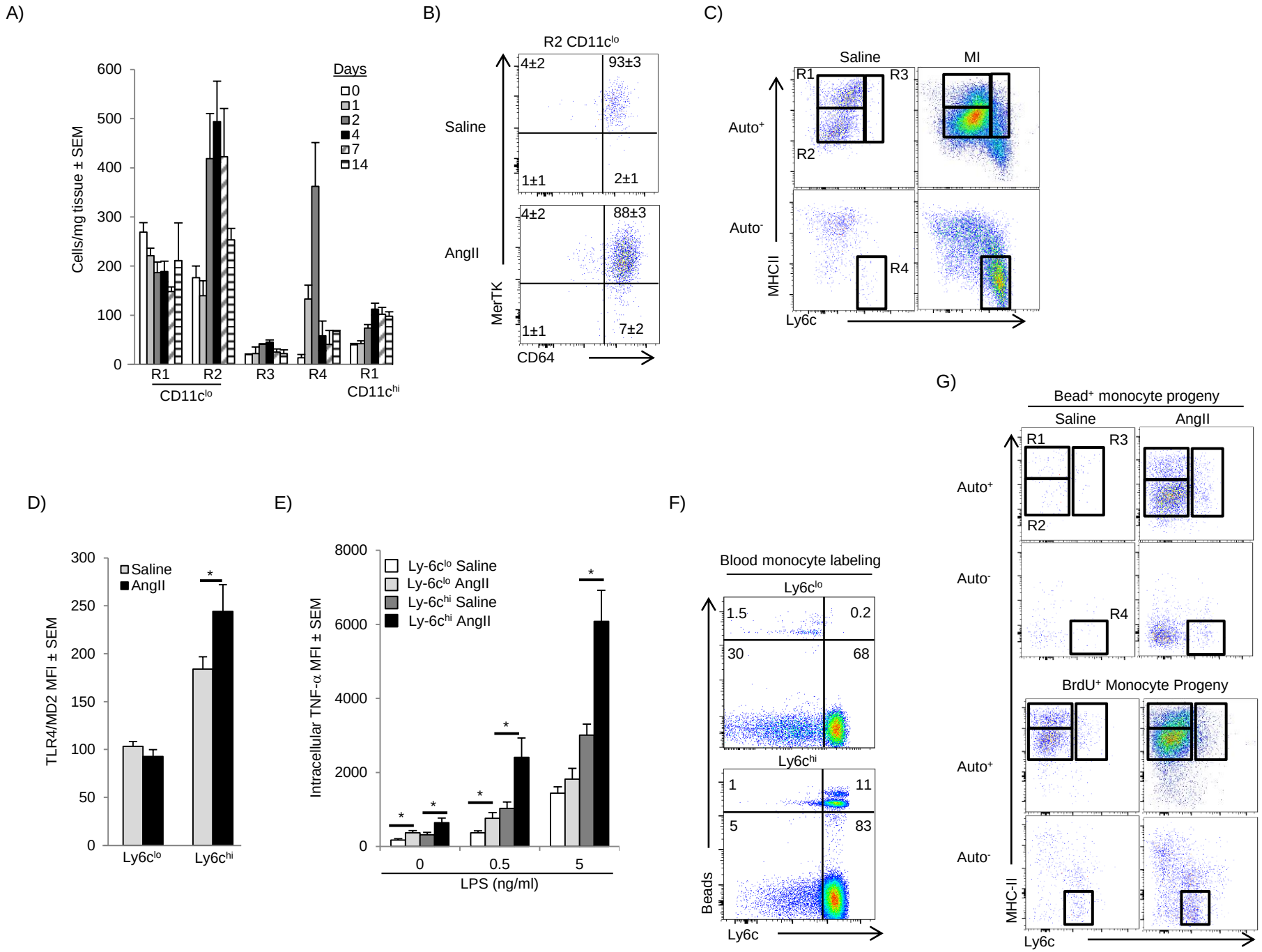
A)
Cells/mg tissue ± SEM
600
500
400
300
200
100
0
Days
0
1
2
4
7
14
R1
R2
R3
R4
R1
CD11c^lo
CD11c^hi
B)
R2 CD11c^lo
Saline
AngII
MerTK
CD64
4±2
93±3
1±1
2±1
4±2
88±3
1±1
7±2
C)
Saline
MI
Auto+
Auto-
MHCII
Ly6c
R1
R2
R3
R4
D)
TLR4/MD2 MFI ± SEM
300
250
200
150
100
50
0
Saline
AngII
*
Ly6c^lo
Ly6c^hi
E)
Intracellular TNF-α MFI ± SEM
8000
6000
4000
2000
0
Ly-6c^lo Saline
Ly-6c^lo AngII
Ly-6c^hi Saline
Ly-6c^hi AngII
*
0
0.5
5
LPS (ng/ml)
F)
Blood monocyte labeling
Ly6c^lo
1.5
0.2
30
68
Ly6c^hi
1
11
5
83
Beads
Ly6c
G)
Bead+ monocyte progeny
Saline
AngII
Auto+
Auto-
R1
R2
R3
R4
BrdU+ Monocyte Progeny
MHC-II
Ly6c

Figure S3.

A)

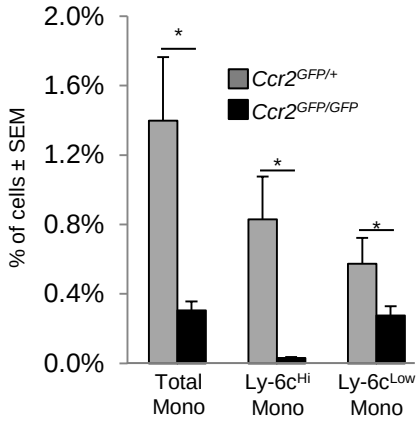

B)

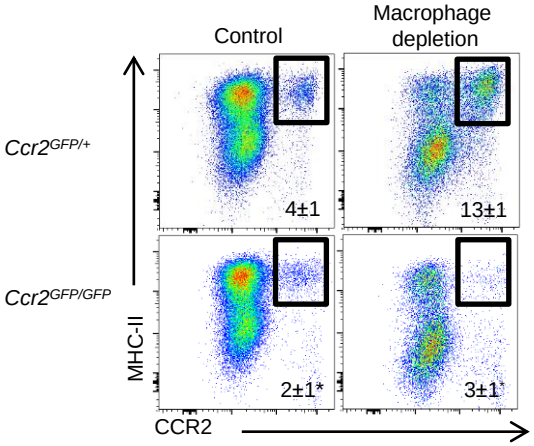

C)

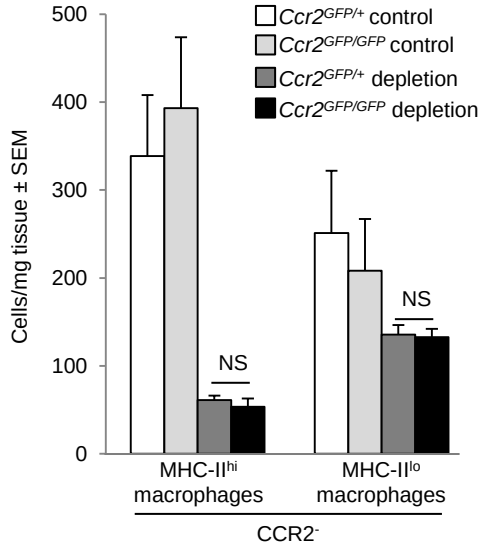

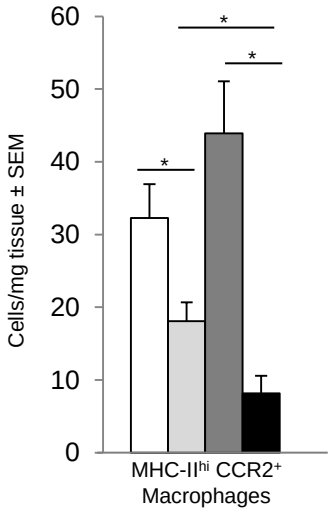

Figure S4.

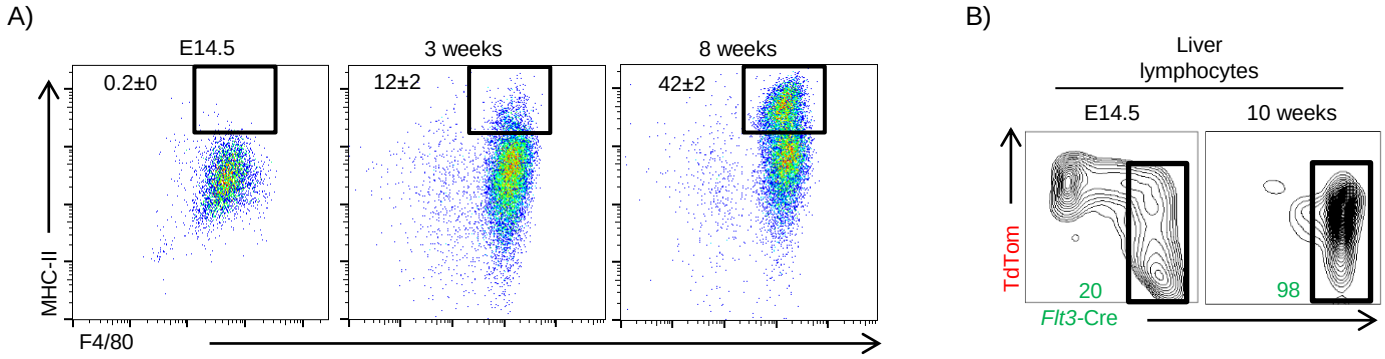
A)
E14.5
3 weeks
8 weeks
0.2±0
12±2
42±2
MHC-II
F4/80
B)
Liver
lymphocytes
E14.5
10 weeks
TdTom
20
98
Flt3-Cre

Figure 5S.

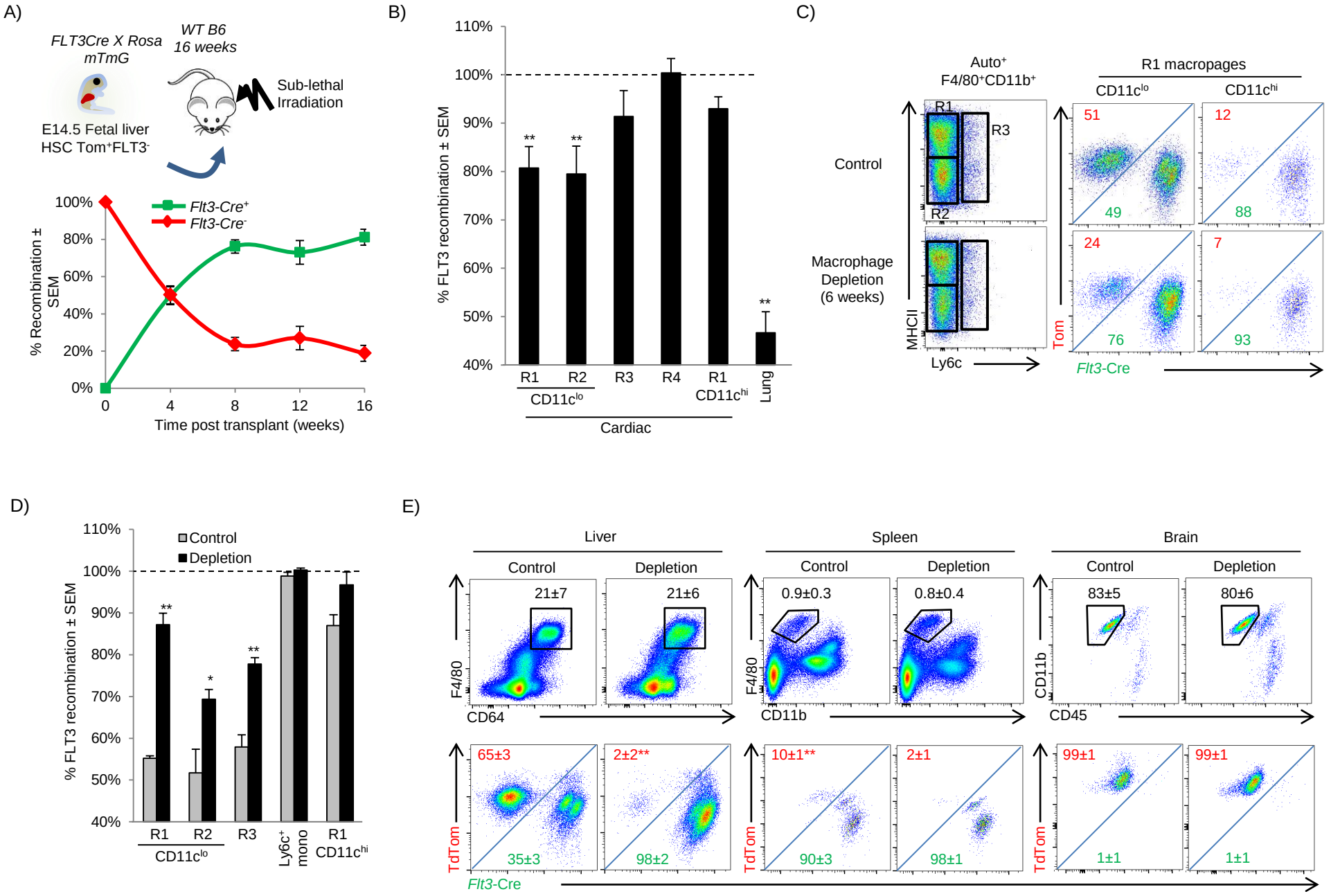
A)
FLT3Cre X Rosa mTmG
WT B6 16 weeks
Sub-lethal Irradiation
E14.5 Fetal liver HSC Tom+FLT3-
Flt3-Cre+
Flt3-Cre-
% Recombination ± SEM
Time post transplant (weeks)
B)
% FLT3 recombination ± SEM
R1 CD11clo
R2
R3
R4
R1 CD11chi
Lung
Cardiac
C)
Auto+ F4/80+CD11b+
R1 macropages
CD11clo
CD11chi
Control
Macrophage Depletion (6 weeks)
R1
R2
R3
MHCII
Ly6c
Tom
Flt3-Cre
51
49
12
88
24
76
7
93
D)
Control
Depletion
% FLT3 recombination ± SEM
R1 CD11clo
R2
R3
Ly6c+ mono
R1 CD11chi
E)
Liver
Spleen
Brain
Control
Depletion
F4/80
CD64
CD11b
CD45
TdTom
Flt3-Cre
21±7
21±6
0.9±0.3
0.8±0.4
83±5
80±6
65±3
35±3
2±2**
98±2
10±1**
90±3
2±1
98±1
99±1
1±1
99±1
1±1

Figure S6

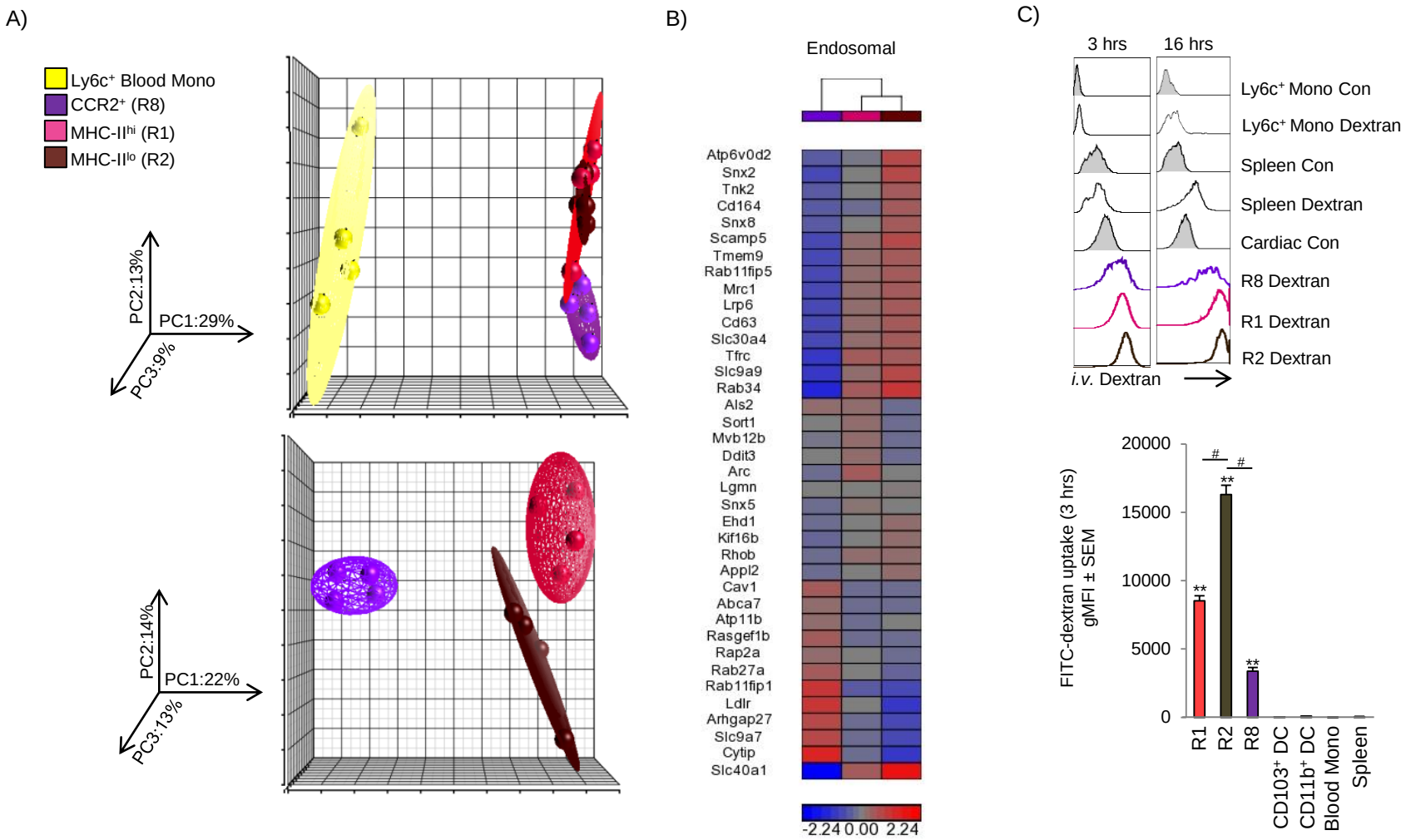
A)
Ly6c+ Blood Mono
CCR2+ (R8)
MHC-IIhi (R1)
MHC-IIlo (R2)
PC2:13%
PC1:29%
PC3:9%
PC2:14%
PC1:22%
PC3:13%
B)
Endosomal
Atp6v0d2
Snx2
Tnk2
Cd164
Snx8
Scamp5
Tmem9
Rab11fip5
Mrc1
Lrp6
Cd63
Slc30a4
Tfrc
Slc9a9
Rab34
Als2
Sort1
Mvb12b
Ddit3
Arc
Lgmn
Snx5
Ehd1
Kif16b
Rhob
Appl2
Cav1
Abca7
Atp11b
Rasgef1b
Rap2a
Rab27a
Rab11fip1
Ldlr
Arhgap27
Slc9a7
Cytip
Slc40a1
-2.24 0.00 2.24
C)
3 hrs
16 hrs
Ly6c+ Mono Con
Ly6c+ Mono Dextran
Spleen Con
Spleen Dextran
Cardiac Con
R8 Dextran
R1 Dextran
R2 Dextran
i.v. Dextran
FITC-dextran uptake (3 hrs)
gMFI ± SEM
20000
15000
10000
5000
0
#
#
**
**
**
R1
R2
R8
CD103+ DC
CD11b+ DC
Blood Mono
Spleen

Figure S7

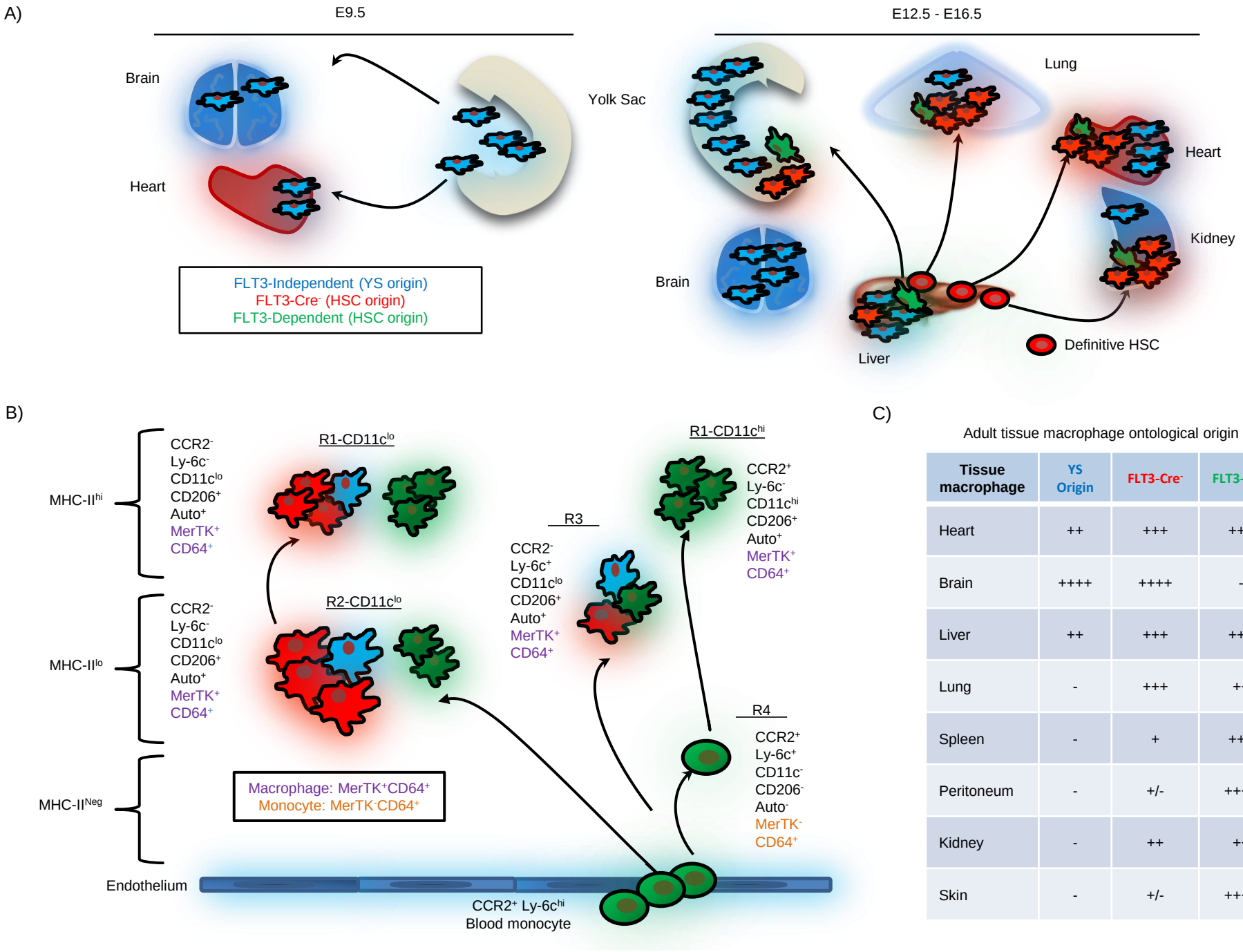

C)

Adult tissue macrophage ontological origin

Tissue macrophage	YS Origin	FLT3-Cre-	FLT3-Cre+
Heart	++	+++	+++
Brain	++++	++++	-
Liver	++	+++	+++
Lung	-	+++	++
Spleen	-	+	+++
Peritoneum	-	+/-	++++
Kidney	-	++	++
Skin	-	+/-	++++

Supplemental Figure Legends

Figure S1. Cardiac macrophage gating strategy (related to Fig 1). Single cell cardiac tissue suspensions were prepared and labeled (see Table S1 for antibody list and Fig 1A). A) $CD45^+$ leukocytes were identified, doublets excluded (by FSC-W vs. FSC-A) and dead cells excluded by DAPI. Live cells were stratified by autofluorescence ($Auto^+$ or $Auto^-$), gated on $F4/80^+CD11b^+$ myeloid cells and then further stratified by MHC-II and Ly6c expression. R1: MHC-II^{hi} macrophages (Orange). R2: MHC-II^{lo} macrophages (blue). R3: $Ly6c^+$ macrophages (black). R4: $Ly6c^{hi}$ monocytes (Red). Size (FSC-A) and granularity (SSC-A) was assessed by flow cytometry of the cardiac macrophage and monocyte populations identified, as was relative F4/80 and CD11b expression in wild type (WT) mice. Neutrophils were identified as $CD45^+CD11b^+Ly6g^+F4/80^-$ (green). B) In order to identify where $CD11b^+$ DCs were in our macrophage gating strategy we analyzed *Zbtb46*$^{GFP/+}$ mice and gated on $CD11b^+$ DCs as in Fig 1D (live $CD45^+Auto^-$MHC-$II^{hi}CD11c^{hi}CD11b^+CD103^-Zbtb46^{hi}$). We backed gated these $CD11b^+$ DCs into our original $Auto^+$ and $Auto^-$ gates and included their relative distribution (F4/80 vs. CD11b) and (MHC-II vs. Ly6c). The MHC-II vs. Ly-6c plots contained cells that were $F4/80^+CD11b^+$. Total $CD45^+$ cells (red) were superimposed with $CD11b^+$ DCs (blue). MHC-II vs. Ly6c plots contain $F4/80^+CD11b^+$ myeloid cells that were gated. $Zbtb46^{hi}$ $CD11b^+$ DCs would not have been carried over from the original F4/80 vs. CD11b gate since they were essentially $F4/80^-$, however we included their position to demonstrate where they would have been located, had they not been excluded earlier.

Figure S2. AngII infusion model to study cardiac monocyte and macrophage dynamics (related to Fig 3). A-B) WT mice were implanted with subcutaneous osmotic mini-pumps that infused angiotensin II (2 mg/kg/day) or saline and cardiac cellular infiltration was assessed from 1-14 days. The regions displayed were gated as in Fig 1A (R1: MHC-II^{hi} macrophages, R2: MHC-II^{lo} macrophages, R3: $Ly6c^+$ macrophages, R4: $Ly6c^+$ monocytes). B) MerTK / CD64 expression on R2 (MHC-II^{lo} $CD11c^{lo}$) macrophages. C) WT mice received surgical myocardial infarction. Cardiac tissue in the infarcted / peri-infarcted area was removed 4 days after instrumentation and cardiac cellular infiltration was assessed. Cells were gated as in Fig 1A. To assess

blood monocyte activation prior to infiltration, we measured Toll like receptor 4 (TLR4)/MD-2 upregulation (D) and intracellular TNF-α production (E) in response to lipopolysaccharide (LPS, 10 ng/ml) in mice that receive either saline containing pumps or AngII (1.5 mg/kg/day) after 4 days. Monocytes were identified as $SSC^{Low}CD115^{+}F4/80^{+}$. F) Representative flow cytometric plots of blood monocytes following either the Ly-$6c^{lo}$ or Ly-$6c^{hi}$ bead labeling protocol (Tacke et al., 2006). G) Saline or AngII was infused using the Ly-$6c^{hi}$ labeling protocol (as in Fig 3B) or BrdU pulsing (2 mg/mouse injected *i.p*. 48 and 24 hrs prior to harvest – as in Fig 3C). All $CD45^{+}F4/80^{+}CD11b^{+}$ $bead^{+}$ or $BrdU^{+}$ cells were gated on and their respective MHC-II and Ly6c profiles are shown (in $Auto^{+}$ and $Auto^{-}$ gates) in order to demonstrate where the progeny of infiltrating cardiac Ly$6c^{hi}$ monocytes reside. At least 2 independent experiments, with 4-7 mice per group. * $P<0.05$.

Figure S3. $CCR2^{+}$ macrophage repopulation was dependent on blood monocyte input (related to Fig 4). A) Percentage of blood monocytes in $Ccr2^{GFP/+}$ and $Ccr2^{GFP/GFP}$ mice. B-C) $Ccr2^{GFP/+}$ and $Ccr2^{GFP/GFP}$ mice were injected with either control liposomes or clodronate liposomes (macrophage depletion). After 7 days the percentage of $CCR2^{+}$MHC-II^{hi} macrophages (B) or the total number of cells (C) is shown. At least 2 independent experiments, with 4-8 mice per group. * $P<0.05$.

Figure S4. Development of cardiac MHC-II^{hi} macrophages after birth (related to Fig 5). A) Development of MHC-II^{hi} macrophages over time. Cardiac macrophages were analyzed at E14.5, and either 3 or 8 weeks after birth in WT mice. Samples were gated on live $CD45^{+}Auto^{+}F4/80^{+}CD11b^{+}Ly6c^{-}CD11c^{-}$ macrophages and the percentage of MHC-II^{hi} resident macrophages is shown. B) Liver samples from *FLT3*-Cre x *Rosa* mTmG mice at E14.5 or 10 weeks of age were gated on $SSC^{lo}CD45^{+}F4/80^{-}CD11b^{-}$ lymphocytes. FLT3-Cre recombination rates are given. 2-4 litters for each time point with pooled tissue from 2-6 embryos per animal were used in embryonic studies. At least 2 independent experiments, with 3-4 mice per group.

Figure S5. Dynamic relationship between FLT3-Cre^{-} tissue macrophagess and FLT3-Cre^{+} blood monocytes after macrophage depletion (related to Fig 5). A) *Flt3-Cre x Rosa* mTmG E14.5 fetal liver Tom^{+}

$CD150^+$ HSCs were sorted and adoptively transplanted into sub-lethally irradiated adult WT mice. Time course of FLT3-driven recombination in the recipient mouse within the engrafted monocyte pool following transplant, from 0-16 weeks. At 0 weeks, $FLT3^-$ (100% $TdTom^+$) HSCs were transplanted and there was increased recombination over time, reaching a plateau at ~8 weeks. B) After HSC transplant as in Fig S5A, cardiac tissue or lung tissue was isolated and macrophage subsets analyzed for FLT3 recombination within the engrafted resident macrophages and blood monocytes. FLT3 recombination was normalized for recombination in blood monocytes. Cardiac samples were gated based on the regions in Fig 1A. Lung macrophages were identified as live $CD45^+CD11c^{hi}F4/80^{hi}CD11b^{lo}SSC^{hi}MHC\text{-}II^{low}$. C-E) *FLT3*-Cre x *Rosa* mTmG mice were injected with either control liposomes (control) or clodronate liposomes (macrophages depletion) and various tissues were harvested 6 weeks later. C-D) Cardiac tissue; E) Liver, spleen and brain. FLT3 recombination rates were normalized for recombination in blood Ly-$6c^{hi}$ monocytes. Liver macrophages were identified as live $CD45^+CD11b^+CD11c^{lo}F4/80^+CD64^+$, splenic macrophages were identified as live $CD45^+F4/80^{hi}D11b^{lo}MHC\text{-}II^{lo}$, and brain microglia were identified as live $CD45^{lo}CD11b^{hi}F4/80^+$. At least 2 independent experiments, with 3-5 mice per group. * $P<0.05$, ** $P<0.01$.

Figure S6. Transcriptional and functional analysis of cardiac macrophages subsets (related to Fig 7). Blood Ly-$6c^{hi}$ monocytes (yellow), MHC-II^{hi} $CCR2^-$ macrophages (R1, Pink) MHC-II^{lo} $CCR2^-$ macrophages (R2, brown) and $CCR2^+$ MHC-II^{hi} macrophages (R8, purple) were sorted from $Ccr2^{GFP/+}$ mice (4 replicates, 2-4 mice per replicate). Global transcriptional array was performed on extracted RNA as described in the materials and methods. A) Principle component analysis including all 4 subsets, and only cardiac macrophages. B) Hierarchal clustering of endosomal genes between cardiac macrophage subsets. C) FITC-dextran was injected *i.v.* and tissue was harvested at either 3 or 16 hours post injection. Dextran uptake was assessed by flow cytometry. Graphed data represent the geometric MFI (gMFI) of FITC dextran in each macrophage subset at 3 hrs, and also includes cardiac DC subsets, which were gated as in Fig 1D. Splenic macrophages were identified as live $CD45^+F4/80^{hi}CD11b^{lo}$. Background fluorescence was subtracted from each subset based on gMFI in

mice that were uninjected. Each experiment was repeated at least twice, n=4-5 per group. ** P <0.01 vs. control. # <0.01 vs. R2 macrophages.

Figure S7. Steady state ontological schematic of cardiac and other resident tissues macrophages (related to all figures). Green indicates a FLT3-HSC dependent origin, red indicates a FLT3-independent origin (FLT3-Cre$^-$), however still derived from HSC fetal monocytes that have not recombined in the embryo due to rapid progression through FLT3$^+$ intermediate (Boyer et al., 2012), and blue indicates a yolk sac (YS) macrophage origin (FLT-3 independent). A) As early as E9.5-E10.5 yolk sac-derived macrophages (CX3CR1^{hi}MHC-II^{lo}Gr-1$^-$) infiltrate the heart, lung and other tissues (Hoeffel et al., 2012; Schulz et al., 2012). From E12.5 → E16.5, increasing numbers of FLT-3 dependent, fetal liver monocyte-derived macrophages (CX3CR1^{lo}Gr1$^{\pm}$MHC-II$^{\pm}$) infiltrate various tissue beds in parallel with yolk sac-derived macrophage populations. Most fetal liver monocyte-derived macrophages transiently pass through a FLT3$^+$ stage, and therefore have very inefficient FLT3-mediated recombination of the reporter (*Rosa* mTmG locus), and remain FLT3-Cre$^-$ despite originating from definitive HSCs. B) Adult myocardium contained four cardiac macrophage populations (regions R1-R4 are as outlined in Fig 1A). Embryonically established, yolk sack and fetal monocyte-derived MHC-II^{lo}CD11c^{lo} macrophages (R1-CD11c^{lo}) develop into MHC-II^{hi}CD11c^{lo} macrophages (R2-CD11c^{lo}) after birth, and replenish through *in situ* proliferation without blood monocyte input. Infiltrating, FLT3-dependent monocytes differentiate into either CCR2$^+$CD11c^{hi}MHC-II^{hi} macrophages (R1-CD11c^{hi}) or into a mixed population of CCR2$^-$Ly6c^{hi}MHC-II^{lo} macrophages (R3). Purple indicates macrophages (MerTK$^+$CD64$^+$) while orange represents monocytes (R4, MerTK$^-$CD64$^+$). C) Relative contributions in adult resident tissues macrophages from yolk sac macrophages, FLT3-Cre$^-$ and FLT3-dependent (FLT3-Cre$^+$) progenitors.

Table S1. Antibodies used.

Target	Clone	Source
CCR2	475301	R&D
Ly6G	1A8	BD Biosciences / Biolegend
CD11b	M1/70	BD Biosciences / Biolegend
B220	RA3-6B2	Biolegend
F4/80	C1:A3-1	BD Biosciences / Biolegend
I-A^b	AF6-120.1	BD Biosciences / Biolegend
Ly6c	AL-21 HK1.4	BD Biosciences / Biolegend
CD115	AFS98	BD Biosciences / Biolegend
MerTK	108928 BAF591	R&D R&D
Steptavidin	PE-Cy7	Biolegend
Gr-1	RB6-8C5	Biolegend
CD206	C068C2	Biolegend
CD11c	N418	BD Biosciences / Biolegend
TLR4/MD2	MTS510	Biolegend
CD64	X54-5/7.1	Biolegend
CD45.1	A20	Biolegend
CD45.2	104	Biolegend
CD45	30-F11	Biolegend
CD103	2E7	Biolegend
CD16/CD32	2.4G2	BD Biosciences
BrdU	Bu20a	Biolegend
Ki67	16A8	Biolegend
TNF-α	MP6-XT22	Biolegend

Table S2: Conserved genes across different tissue macrophage subsets

MHC-II^{lo} CCR2^{-} macrophages			MHC-II^{hi} CCR2^{-} macrophages			CCR2^{+} MHC-II^{hi} macrophages		
Gene	P value	Fold	Gene	P value	Fold	Gene	P value	Fold
C1qc	1.4E-14	1446	C1qc	1.6E-14	1318	C1qc	4.6E-14	1108
Pmp22	1.3E-12	407	Pmp22	1.5E-12	365	C1qa	4.0E-11	268
C1qa	4.7E-11	358	Pla2g2d	1.6E-07	360	Cd81	3.5E-10	261
Fcna	1.0E-09	323	C1qa	5.2E-11	333	Ccl12	1.9E-10	220
Cd81	2.5E-10	293	Cd81	2.1E-10	329	Mb	1.5E-11	171
Pla2g2d	2.4E-07	282	Ccl12	8.2E-11	296	Rgs1	3.0E-10	143
Lyve1	3.3E-10	263	Slco2b1	2.4E-10	280	C1qb	3.9E-11	113
Igf1	1.6E-12	255	Igf1	2.3E-12	200	Slco2b1	7.4E-10	109
Slco2b1	3.2E-10	230	Stab1	8.8E-11	166	Mmp12	6.2E-10	108
Mrc1	7.8E-10	182	Cd63	4.8E-12	162	Mertk	3.5E-10	94
Cd63	4.4E-12	171	Mrc1	1.3E-09	138	Ccl4	3.4E-08	94
Mertk	1.2E-10	148	Mertk	1.3E-10	138	Mrc1	4.5E-09	83
Vsig4	2.1E-08	134	Fcna	6.2E-09	113	Cd63	2.8E-11	82
C1qb	5.9E-11	120	Lyve1	1.6E-09	106	Stab1	3.5E-10	73
Fn1	5.7E-07	-199	Chi3l3	4.0E-06	-196	Plac8	1.5E-05	-39
F10	1.0E-07	-209	Sell	5.3E-07	-199	Sell	5.3E-06	-59
Chi3l3	2.7E-06	-252	F10	7.4E-08	-254	Hba-a1	1.1E-05	-60
Napsa	2.4E-08	-254	Plac8	5.3E-07	-317	Hba-a2	7.1E-06	-81
Plac8	4.8E-07	-337	Ear2	4.1E-13	-417	Hbb-b1	1.3E-06	-104
Ear2	4.2E-13	-409	Fn1	1.1E-07	-586	Hbb-b2	4.6E-07	-130

Lung macrophages			Microglia			Peritoneal macrophages		
Gene	P value	Fold	Gene	P value	Fold	Gene	P value	Fold
Ear1	1.48E-12	249	C1qc	1.0E-15	132	Vsig4	1.3E-07	162
Mertk	1.13E-09	56	C1qb	6.9E-16	79	C1qc	1.5E-15	115
Dab2	1.19E-09	44	C1qa	5.6E-15	77	C1qa	1.2E-14	62
Mrc1	4.33E-09	37	Slco2b1	3.7E-14	74	C1qb	4.1E-15	48
Myo1e	2.08E-11	29	Cd81	1.4E-15	69	Pmp22	1.3E-11	41
Spp1	8.09E-08	28	Mertk	1.9E-09	48	Ephx1	1.0E-10	30
Ear2	9.38E-08	25	Pmp22	1.5E-11	39	Fgfr1	5.7E-13	29
Rgs1	5.86E-06	17	Rgs1	6.8E-07	30	Mertk	2.7E-08	24
Cd81	6.48E-13	16	Ccl12	5.9E-11	29	Fcna	7.4E-10	24
Slco2b1	3.42E-11	15	Stab1	1.8E-07	14	Dab2	3.4E-08	19
Rhoc	4.45E-11	11	Ccl4	1.2E-09	12	Cd81	3.0E-13	19
Cd63	3.69E-10	11	Cxcl16	1.1E-09	9	Myo1e	8.5E-10	13
Mt2	1.63E-07	7	Ephx1	7.3E-08	8	Igf1	4.3E-09	8
Cttnbp2nl	5.49E-06	6	Cd63	2.3E-09	8	Lyve1	6.1E-06	6
Hp	2.99E-10	-39	F10	1.4E-10	-17	Sell	8.5E-07	-8
I830127L07Rik	1.89E-12	-56	Sell	1.5E-10	-49	Ear2	8.2E-07	-15
Sell	3.62E-11	-74	Plac8	1.0E-09	-52	Chi3l3	1.3E-07	-16
Serpinb10	1.04E-11	-89	Sirpb1b	7.4E-13	-75	Sirpb1b	3.1E-10	-17
Plac8	1.26E-10	-99	Chi3l3	1.4E-10	-103	Mmp8	1.5E-12	-85
Ifitm6	2.16E-11	-127	Fn1	6.3E-11	-117	Plac8	1.3E-10	-97

3/6 populations
4/6 populations
5/6 populations
6/6 populations

Table S3: GO Enrichment analysis between cardiac macrophage subsets

CCR2^{+} vs MHC-II^{hi}			CCR2^{+} vs MHC-II^{lo}			MHC-II^{hi} vs. MHC-II^{lo}		
Name	**Enrichment**	**P value**	**Name**	**Enrichment**	**P value**	**Name**	**Enrichment**	**P value**
regulation of immune system process	17.3766	$2.8x10^{-8}$	**immune system process**	30.3062	$6.9x10^{-14}$	**antigen processing and presentation of exogenous peptide antigen via MHC class II**	20.8933	$8.4x10^{-10}$
positive regulation of immune system process	15.7848	$1.4x10^{-7}$	**regulation of immune system process**	28.2021	$5.7x10^{-13}$	**antigen processing and presentation of peptide antigen via MHC class II**	20.2968	$1.5x10^{-9}$
regulation of immune response	15.4374	$1.9x10^{-7}$	**regulation of response to stimulus**	25.5101	$8.3x10^{-12}$	**antigen processing and presentation of peptide or polysaccharide antigen via MHC class II**	19.7786	$2.6x10^{-9}$
immune system process	14.8988	$3.4x10^{-7}$	**regulation of defense response**	25.1818	$1.2x10^{-11}$	**antigen processing and presentation of exogenous peptide antigen**	19.1099	$5.0x10^{-9}$
regulation of T cell activation	14.0558	$7.9x10^{-7}$	**regulation of T cell activation**	23.6557	$5.3x10^{-11}$	**antigen processing and presentation of exogenous antigen**	18.1979	$1.3x10^{-8}$
regulation of response to stimulus	12.5639	$3.5x10^{-6}$	**regulation of immune response**	22.2452	$2.2x10^{-10}$	**antigen processing and presentation of peptide antigen**	16.8336	$4.9x10^{-8}$
cellular component movement	12.5189	$3.7x10^{-6}$	**positive regulation of response to stimulus**	22.0174	$2.7x10^{-10}$	**immune response**	15.5869	$1.7x10^{-8}$
regulation of T cell proliferation	12.3021	$4.5x10^{-6}$	**immune response**	21.7299	$3.7x10^{-10}$	**antigen processing and presentation**	14.9451	$3.2x10^{-7}$
positive regulation of immune response	12.1926	$5.1x10^{-6}$	**regulation of inflammatory response**	21.3868	$5.2x10^{-10}$	**chaperone mediated protein folding requiring cofactor**	14.8946	$3.4x10^{-7}$
regulation of inflammatory response	11.6302	$8.9x10^{-6}$	**antigen processing and presentation of exogenous peptide antigen via MHC class II**	20.9729	$7.8x10^{-10}$	**'de novo' posttranslational protein folding**	14.09	$7.6x10^{-8}$

Supplemental Experimental Procedures

Mice.

6-12 week old C57BL/6J mice (The Jackson Laboratory) were used for this study and were bred in our animal facility prior to use. *Cx3cr1*$^{GFP/+}$C57BL/6 were kindly provided by Dr. Daniel Link (Jung et al., 2000). *Zbtb46*$^{GFP/+}$ mice were provided by Dr. Kenneth M Murphy and have been previously described (Qi et al., 2009; Tailor et al., 2008; Xu et al., 2012; Edelson et al., 2011; Satpathy et al., 2012). *Flt3*-Cre mice were a kind gift from Dr. Thomas Boehm and were crossed with *Rosa* mTmG C57BL/6 reporter mice (Jackson) (Boyer et al., 2011). *Ccr2*-GFP mice were generated by insertion of GFP under control of the native *CCR2* promoter (Satpathy et al., 2013). *Ccr2*$^{GFP/GFP}$ mice had reduced blood Ly6c^{hi} as has previously been described for *Ccr2*$^{-/-}$ mice (Serbina and Pamer, 2006). *CD115-Mer-iCre-Mer* mice were provided by Dr. Jeffry Pollard (Qian et al., 2011) and were crossed with the *Rosa* mTmG reporter. Tamoxifen (2 mg) was gavaged in 100 μl of corn oil at E8.5 to label yolk sac macrophages (Schulz et al., 2012). *Mlc2V-Cre Rosa tdTomato* mice express the TdTom reporter only in cardiac ventricular myocardium (Chen et al., 1998), and were a kind gift from Dr. Stacey Rentschler. All mice were bred and maintained at the Washington University School of Medicine and experimental procedures were done in accordance with the animal-use oversight committees.

Tissue isolation.

Mice were euthanized by CO_2 fixation, blood was isolated into heparinized syringes. Hearts were then perfused with 20 ml of cold PBS. Hearts, lungs, kidneys, brains and livers were minced finely and digested with shaking for 1 hr at 37^{o}C in DMEM containing collagenase I, collagenase XI, DNase I, and hyaluronidase (Sigma) enzymes (Nahrendorf et al., 2007). Experiments in which MerTK was used required digestion in Collagenase D (Roche) and DNAse I for 30 min at 37^{o}C. The digested material from heart, lungs and kidneys was filtered through 40 μM filters and pelleted by centrifugation (400xg for 5 min at 4^{o}C) in HBSS supplemented with 2% FCS + 0.2% BSA. Red blood cells were lysed in ACK lysis buffer (InVitrogen) and then resuspended in FACS buffer (PBS containing 2% FCS and 2 mM EDTA). Liver and brain were filtered and resuspended into 40%

Percoll, and the brain was layered over 80% percoll prior to centrifugation. Brian microglial were collected at the interface, washed and resuspended in FACS buffer. Liver pellets were resuspended, remaining RBCs were lysed as above and samples resuspended in FACS buffer. Skin was shaved, excised cut and floated in Liberase (400 μg/ml in RPMI) epidermis side up for 30 min at 37^{o}C. The tissue was minced and broken up by pipetting, filtered through a 100 μM strainer, washed with RPMI and resuspended in FACS buffer. Spleens were removed, minced and triturated through 40 μM filters in HBSS, RBC lysed as above and resuspended in FACS solution. Peritoneal lavage was performed in naive mice with ice cold HBSS + 0.2% BSA. Peritoneal cells were spun down and RBCs were lysed. Blood was collected into heparinized syringes, RBCs were lysed and resuspended in FACS buffer. Embryonic tissue age was estimated by assessing for the presence of vaginal plug. Tissues were removed in cold HBSS, minced and digested as above for 45 min (except the YS, which was digest for 90 min), and resuspended in FACS buffer. To assess tissue IL-1β production, cardiac tissue was isolated, disrupted by dounce homogenization in ice cold lysis buffer (Cell Lysis Buffer, Cell Signaling). Cellular debris was removed by centrifugation (12,000 x g, 20 min, 4^{o}C). Cardiac tissue supernatant protein content was determined (Pierce), and 500 μg of each sample was used to detect IL-1β by commercial ELISA assay (R&D systems).

Antibodies and flow cytometry.

All antibodies used in this study are listed in supplemental table 1. All flow cytometric analysis was done on either an LSR Fortessa or FACS Canto II. Samples were blocked with Fc block (BD Bioscience) for 15 min prior to labeling for 30 min at 4^{o}C with antibodies and washed in FACS buffer. After gating on CD45^{+} cells, doublets were excluded and live cells were analyzed (DAPI exclusion). Total cell counts were estimated by the total number of events / sample per mg of tissue. For intracellular staining, samples were stimulated in RPMI + 10% FCS (Gibco) with LPS for 3 hours in the presence of monensin in non-adherent plates. Cells were collected, washed and cell surface molecules were labeled as above. Antibodies were washed off, the samples were fixed/permeabilized (CytoFix/CytoPerm BD Bioscience), and then labeled with anti-TNF-α. For

proliferation experiments, 2 mg of BrdU (Sigma) was injected *i.p.* 2 hrs prior to harvest and for Ly-6c^{Hi} labeling experiments, 1 mg of BrdU was injected daily for the indicated time points (Zhu et al., 2009). To detect intracellular BrdU, the BD Bioscience Cytofix/cytoperm technique was used. Briefly, cells were fixed after cell surface staining as above, DNA was digested for 1 hour with DNase (Sigma), and then samples were labeled with anti-BrdU antibody. Clodronate-loaded liposomes were produced as previously described and contained 18 mg of clodronate / ml of beads (Seiler et al., 1997). 100 ul / 30 g mouse was injected *i.v.* for depletion studies. Peripheral blood Ly-6c^{Hi} and Ly-6c^{Low} monocytes were labeled *in vivo* with 1 μm fluorescent microspheres (Polyscience, PA) as previously described (Tacke et al., 2007). To assess macrophage antigen sampling, 100 μL of 0.2% FITC-dextran (70 kDa, Sigma) was injected into the tail vein *i.v.*. Cardiac tissue, blood and spleen was isolated at the indicated time points and processed as above. Cardiac tissue macrophages were gated as indicated in the figure legends. The four macrohage populations were gated as in Fig 1 and summarized in Fig S7. Cardiac macrophages were all live CD45^{+}F4/80^{+} CD11b^{+}Auto^{+}. Total cardiac macrophages were further stratified by the following gating: R1-CD11c^{lo}: CD11c^{lo}CD206^{+}CX3CR1^{hi}Ly6c^{-} CCR2^{-}MHC-II^{hi}, R2-CD11c^{lo}: CD11c^{lo}CD206^{+}CX3CR1^{int}Ly6c^{-}CCR2^{-}MHC-II^{lo}; R3-Ly6c^{+}: CD11c^{lo}CD206^{+} CX3CR1^{hi}Ly6c^{+}CCR2^{-}MHC-II^{+}; R1-CD11c^{hi}: CD11c^{hi}CD206^{+}CX3CR1^{hi}Ly6c^{-}CCR2^{+}MHC-II^{hi}CD103^{-}. Other resident tissue macrophages were gated as follows. Lung: CD45^{+}CD11c^{hi}F4/80^{hi}CD11b^{lo} SSC^{hi}MHC-II^{lo}. Brain Microglia: CD45^{lo}CD11b^{hi}F4/80^{+}. Kidney: CD45^{+}F4/80^{hi}CD11b$^{lo\text{-}int}$, splenic: CD45^{+}F4/80^{hi}CD11b^{lo}; Liver: CD45^{+}CD11b^{hi}F4/80^{hi}CD64^{+}CD11c^{lo}; Skin: CD45^{+}MerTK^{+} CD64^{+}.

Cell sorting and adoptive transfer.

Cell sorting was performed using AriaII instrumentation (BD Bioscience). To sort macrophage populations in *Ccr2*$^{GFP/+}$ mice, we altered our digestion protocol to minimize activation. Minced cardiac tissue was digested for only 20 min in Collagenase D (Roche) and DNase I (as above). RBCs were lysed for 3 min. Cells were gated on live (DAPI^{-}), CD45^{+}Auto^{+}F4/80^{+}CD11b^{+} Ly6c^{-}CD64^{+}MerTK^{+} macrophages and then stratified by MHC-II and CCR2 expression as in Fig 7A into the 3 three sorted macrophage populations. Blood was isolated

through cardiac puncture as described above. $Ly6c^{hi}$ blood monocytes were identified and sorted as live ($DAPI^-$), $CD45^+F4/80^+CD115^+SSC^{lo}Ly6c^{hi}$. All samples were sorted directly into either RPMI + 50% bovine serum for functional studies or into Trizol for RNA extraction (see below). Cytospins of the live sorted cells were prepared, stained with Hema 3 solution (Fischer Scientific) visualized at 20x (Zeiss Axioscope). Cross sectional area was calculated on AxioVision LE software. To sort fetal liver HSCs, E14.5 livers from *Flt3*-Cre x *Rosa* mTmG embryos were removed, dissociated on ice using frosted cover slips and 200 $CD150^{hi}$ Tom^+ KLS (c-$Kit^+Lin^-Sca\text{-}1^+$) HSCs were adoptively transferred into sublethally irradiated (770 rads) male 8-10 week old C57BL/6 mice. Peripheral blood chimerism was assessed every 4 weeks for 16 weeks by analysis of fluorescence profiles within blood leukocyte populations (either Tom^+ and GFP^+). Lung and cardiac tissue was harvested, engraftment percentages were calculated for each cellular subset by flow cytometry 16 weeks following adoptive transplant and normalized for engraftment rates in blood $Ly6c^{hi}$ monocytes.

Osmotic Mini-Pump Implantation, Myocardial infarction surgery and Parabiosis.

For osmotic mini-pump (Alzet) implantation, mice with anesthetized with ketamine/xylazine, the back was shaved and mini pumps containing either saline or angiotensin II (AngII) (Bachem, 1.5 – 2.0 mg/kg/day) were implanted. The incisions were closed with silk sutures. Complete left anterior descending aorta occlusion was performed as previously described (Sondergaard et al., 2010). C57BL/6J and B6-Ly5.1 female mice controlled for age and weight were parabiosed. The mice were joined at the elbow and knee with dissolvable sutures and the incision was closed with wound clips. Postoperative care included administration of buprenex compound for pain management, 5% dextrose and 0.9% sodium chloride, nutritional gel packs provided in each cage and antibiotics (Sulfatrim) provided in the drinking water (Peng et al., 2013).

Transcriptional Array

RNA from cardiac macrophages and blood monocytes was extracted from trizol samples using the qiagen micro-kit (Qiagen). Total RNA concentration and quality was determined by Agilent 2100 bioanalyzer (Agilent

Technologies) according to manufacturer's recommendations. RNA transcripts were first amplified by WTA2 kit (Sigma Aldrich). 1 ng of total RNA was amplified according to manufacturer's protocol. cDNAs were chemically labeled with Kreatech ULS labeling kit (Kreatech Diagnostics). Per reaction, 2.5 μg of DNA was mixed with Kreatech labeling buffer and Kreatech cy5-ULS. The reactions were incubated at 85^{o}C for 15 minutes in the dark and placed on ice for 3 minutes. Labeled DNAs were purified with QIAquick PCR purification columns (Qiagen Sciences). Labeled DNAs were quantitated on a Nanodrop spectrophotometer. 2 μg of each labeled DNA was suspended in Agilent 2X Gene Expression hybridization buffer, Agilent 10X Blocking agent and Kreatech Kreablock. The hybridization solutions were applied to Agilent Mouse 4x44K microarrays. Hybridization was carried out at 65^{o}C for 20 hours. Washing procedures were carried out according to Agilent gene expression protocols. Slides were scanned on an Agilent SureScan microarray scanner to detect Cy5 fluorescence. Gridding and analysis of images was performed using Agilent Feature Extraction v10.7.3.1. Background subtracted, log transformed, quantile normalized data were analyzed using ANOVA testing with contrasts (Partek GS, Partek, St. Louis, MO). For all pairwise tests we set our threshold at a two-fold change with a 99% confidence interval by moderated t test with Benjamini-Hochberg False Discovery Rate analysis. Hierarchical clustering analysis, heat map plot generation (without scaling) and gene ontology was performed using Partek GS. We imported gene array data (background subtracted, log transformed, quantile normalized) from Immgen (http://www.immgen.org/) for brain microglia (data files 111383, 11384, 113835), Lung MΦs (data files 87584, 87585, 87586), Peritoneal F4/80^{Hi} MΦs (data files 105224, 105225, 105226) and blood Ly6c^{Hi}MHC-II^{Neg} monocytes (data files 96439, 96440, 96441) (Heng and Painter, 2008). We compared differentially expressed genes between blood Ly6c^{Hi} monocytes and each MΦ subsets as indicated above.

Cardiomyocyte Phagocytosis Assay

For cardiomyocyte labeling, hearts from WT mice were removed, digested as indicated above and resuspended in RPMI+10% FCS. Heart samples were incubated for 1 hour at 37^{o}C in standard tissue culture plates. Non-adherent apoptotic / necrotic cells (DAPI^{+} ~50%, data not shown) were removed and permanently labeled with

CellVue Claret Far Red Fluorescent Cell Linker Kit (Sigma) as per the manufacturer's instructions, and resuspended in RPMI+ 10% FCS. Separately, cardiac single cell suspensions or splenocytes from *Ccr2*$^{GFP/+}$ mice were labeled with cell surface antibodies at 4^{o}C as described above, washed and resuspended in RPMI + 10% FCS. CellVue labeled cardiomyocytes were incubated with antibody-labeled cardiac and splenic samples at either 4^{o}C or 37^{o}C for 4 hours in order to distinguish cell surface binding (4^{o}C) from active phagocytosis (37^{o}C) in non-adherent tissue culture plates (Mounier et al., 2013). Cardiac and splenic samples were gated to identify MΦs, and the percentage of cells that were CellVue^{+} was determined by flow cytometry.

Antigen Presenting Cell Assay

The ability of cardiac MΦ to act as antigen presenting cells was assessed to Listeriolysin O (LLO) peptide and protein as described (Carrero et al., 2012). Briefly, cardiac MΦs and Ly-6c^{Hi} monocytes were sorted into DMEM + 10% fetal calf serum. 5-7 mice were pooled and the assay was run in duplicate. 2x10^{4} cells were plated and incubated with LLO peptide (190-201) or a variant of the intact LLO protein (LLOWW) that is none-hemolytic for 2 hours at 37^{o}C (Carrero et al., 2012). 2x10^{5} irradiated splenocytes served a positive control. T cell hybridoma specific for LLO(190-201) (5×10^{4} cells) was added for ~16 hrs. Culture supernatants were tested for IL-2 production by CTLL-2 proliferation assay using ^{3}H-thymidine incorporation. All antigen presentation assays were performed in 200-µL final volume in 96-well tissue culture coated flat-bottom plates (Corning, Lowell, MA).

Statistics

All data are presented as mean ± SEM. Two-tailed Student's t test was used for comparisons between experimental groups. Significant differences were defined at $P < 0.05$.

Supplemental References

Boyer,S.W., Beaudin,A.E., and Forsberg,E.C. (2012). Mapping differentiation pathways from hematopoietic stem cells using Flk2/Flt3 lineage tracing. Cell Cycle *11*, 3180-3188.

Boyer,S.W., Schroeder,A.V., Smith-Berdan,S., and Forsberg,E.C. (2011). All hematopoietic cells develop from hematopoietic stem cells through Flk2/Flt3-positive progenitor cells. Cell Stem Cell *9*, 64-73.

Carrero,J.A., Vivanco-Cid,H., and Unanue,E.R. (2012). Listeriolysin o is strongly immunogenic independently of its cytotoxic activity. PLoS. One. *7*, e32310.

Chen,J., Kubalak,S.W., and Chien,K.R. (1998). Ventricular muscle-restricted targeting of the RXRalpha gene reveals a non-cell-autonomous requirement in cardiac chamber morphogenesis. Development *125*, 1943-1949.

Edelson,B.T., Bradstreet,T.R., KC,W., Hildner,K., Herzog,J.W., Sim,J., Russell,J.H., Murphy,T.L., Unanue,E.R., and Murphy,K.M. (2011). Batf3-dependent CD11b(low/-) peripheral dendritic cells are GM-CSF-independent and are not required for Th cell priming after subcutaneous immunization. PLoS. One. *6*, e25660.

Heng,T.S. and Painter,M.W. (2008). The Immunological Genome Project: networks of gene expression in immune cells. Nat. Immunol. *9*, 1091-1094.

Hoeffel,G., Wang,Y., Greter,M., See,P., Teo,P., Malleret,B., Leboeuf,M., Low,D., Oller,G., Almeida,F., Choy,S.H., Grisotto,M., Renia,L., Conway,S.J., Stanley,E.R., Chan,J.K., Ng,L.G., Samokhvalov,I.M., Merad,M., and Ginhoux,F. (2012). Adult Langerhans cells derive predominantly from embryonic fetal liver monocytes with a minor contribution of yolk sac-derived macrophages. J. Exp. Med. *209*, 1167-1181.

Jung,S., Aliberti,J., Graemmel,P., Sunshine,M.J., Kreutzberg,G.W., Sher,A., and Littman,D.R. (2000). Analysis of fractalkine receptor CX(3)CR1 function by targeted deletion and green fluorescent protein reporter gene insertion. Mol. Cell Biol. *20*, 4106-4114.

Mounier,R., Theret,M., Arnold,L., Cuvellier,S., Bultot,L., Goransson,O., Sanz,N., Ferry,A., Sakamoto,K., Foretz,M., Viollet,B., and Chazaud,B. (2013). AMPKalpha1 regulates macrophage skewing at the time of resolution of inflammation during skeletal muscle regeneration. Cell Metab *18*, 251-264.

Nahrendorf,M., Swirski,F.K., Aikawa,E., Stangenberg,L., Wurdinger,T., Figueiredo,J.L., Libby,P., Weissleder,R., and Pittet,M.J. (2007). The healing myocardium sequentially mobilizes two monocyte subsets with divergent and complementary functions. J. Exp. Med. *204*, 3037-3047.

Peng,H., Jiang,X., Chen,Y., Sojka,D.K., Wei,H., Gao,X., Sun,R., Yokoyama,W.M., and Tian,Z. (2013). Liver-resident NK cells confer adaptive immunity in skin-contact inflammation. J. Clin. Invest *123*, 1444-1456.

Qi,C.F., Li,Z., Raffeld,M., Wang,H., Kovalchuk,A.L., and Morse,H.C., III (2009). Differential expression of IRF8 in subsets of macrophages and dendritic cells and effects of IRF8 deficiency on splenic B cell and macrophage compartments. Immunol. Res. *45*, 62-74.

Qian,B.Z., Li,J., Zhang,H., Kitamura,T., Zhang,J., Campion,L.R., Kaiser,E.A., Snyder,L.A., and Pollard,J.W. (2011). CCL2 recruits inflammatory monocytes to facilitate breast-tumour metastasis. Nature *475*, 222-225.

Satpathy, A. T., Briseno, C. G., Lee, J. S., Ng, D., Manieri, N. A., KC, W., Wu, X., Thomas, S. R., Lee, W. L., Turkoz, M., McDonald, K. G., Meredith, M. M., Song, C, Guidos, C. J., Newberry, R. D., Ouyang, W, Murphy, T. L., Stappenbeck, T. S., Gommerman, J. L., Nussenzweig, M. C., Colonna, M., Kopan, R., and Muprhy, K. M. Notch2-dependent classical dendritic cells orchestrate intestinal immunity against attaching and effacing bacterial pathogens. Nat.Immunol. In Press. 2013.
Ref Type: Generic

Satpathy,A.T., KC,W., Albring,J.C., Edelson,B.T., Kretzer,N.M., Bhattacharya,D., Murphy,T.L., and Murphy,K.M. (2012). Zbtb46 expression distinguishes classical dendritic cells and their committed progenitors from other immune lineages. J. Exp. Med. *209*, 1135-1152.

Schulz,C., Gomez,P.E., Chorro,L., Szabo-Rogers,H., Cagnard,N., Kierdorf,K., Prinz,M., Wu,B., Jacobsen,S.E., Pollard,J.W., Frampton,J., Liu,K.J., and Geissmann,F. (2012). A lineage of myeloid cells independent of Myb and hematopoietic stem cells. Science *336*, 86-90.

Seiler,P., Aichele,P., Odermatt,B., Hengartner,H., Zinkernagel,R.M., and Schwendener,R.A. (1997). Crucial role of marginal zone macrophages and marginal zone metallophils in the clearance of lymphocytic choriomeningitis virus infection. Eur. J. Immunol. *27*, 2626-2633.

Serbina,N.V. and Pamer,E.G. (2006). Monocyte emigration from bone marrow during bacterial infection requires signals mediated by chemokine receptor CCR2. Nat. Immunol. *7*, 311-317.

Sondergaard,C.S., Hess,D.A., Maxwell,D.J., Weinheimer,C., Rosova,I., Creer,M.H., Piwnica-Worms,D., Kovacs,A., Pedersen,L., and Nolta,J.A. (2010). Human cord blood progenitors with high aldehyde dehydrogenase activity improve vascular density in a model of acute myocardial infarction. J. Transl. Med. *8*, 24.

Tacke,F., Alvarez,D., Kaplan,T.J., Jakubzick,C., Spanbroek,R., Llodra,J., Garin,A., Liu,J., Mack,M., van,R.N., Lira,S.A., Habenicht,A.J., and Randolph,G.J. (2007). Monocyte subsets differentially employ CCR2, CCR5, and CX3CR1 to accumulate within atherosclerotic plaques. J. Clin. Invest *117*, 185-194.

Tacke,F., Ginhoux,F., Jakubzick,C., van,R.N., Merad,M., and Randolph,G.J. (2006). Immature monocytes acquire antigens from other cells in the bone marrow and present them to T cells after maturing in the periphery. J. Exp. Med. *203*, 583-597.

Tailor,P., Tamura,T., Morse,H.C., III, and Ozato,K. (2008). The BXH2 mutation in IRF8 differentially impairs dendritic cell subset development in the mouse. Blood *111*, 1942-1945.

Xu,H., Zhu,J., Smith,S., Foldi,J., Zhao,B., Chung,A.Y., Outtz,H., Kitajewski,J., Shi,C., Weber,S., Saftig,P., Li,Y., Ozato,K., Blobel,C.P., Ivashkiv,L.B., and Hu,X. (2012). Notch-RBP-J signaling regulates the transcription factor IRF8 to promote inflammatory macrophage polarization. Nat. Immunol. *13*, 642-650.

Zhu,S.N., Chen,M., Jongstra-Bilen,J., and Cybulsky,M.I. (2009). GM-CSF regulates intimal cell proliferation in nascent atherosclerotic lesions. J. Exp. Med. *206*, 2141-2149.